

**Extracellular vesicles from *Aggregatibacter actinomycetemcomitans* exhibit potential antitumorigenic effects in oral cancer: A comparative in vitro study**

Marjut Metsäniitty<sup>1</sup>, Shrabon Hasnat<sup>1</sup>, Carina Öhman<sup>2</sup>, Tuula Salo<sup>1</sup>, Kari K. Eklund,<sup>3,4</sup> Jan Oscarsson<sup>2</sup>, Abdelhakim Salem<sup>1,3,#</sup>

<sup>1</sup>Department of Oral and Maxillofacial Diseases, Clincum, University of Helsinki, 00014 Helsinki, Finland

<sup>2</sup>Oral Microbiology, Department of Odontology, Umeå University, 90187 Umeå, Sweden

<sup>3</sup>Department of Rheumatology, University of Helsinki and Helsinki University Hospital, Helsinki, 00014, Finland

<sup>4</sup>Translational Immunology Research Program (TRIMM), Research Program Unit (RPU), University of Helsinki, 00014 Helsinki, Finland

#Corresponding author: Assoc. Professor Abdelhakim Salem (E-mail: [abdelhakim.salem@helsinki.fi](mailto:abdelhakim.salem@helsinki.fi)),  
ORCID: 0000-0002-9455-3823

**Supplementary figures**

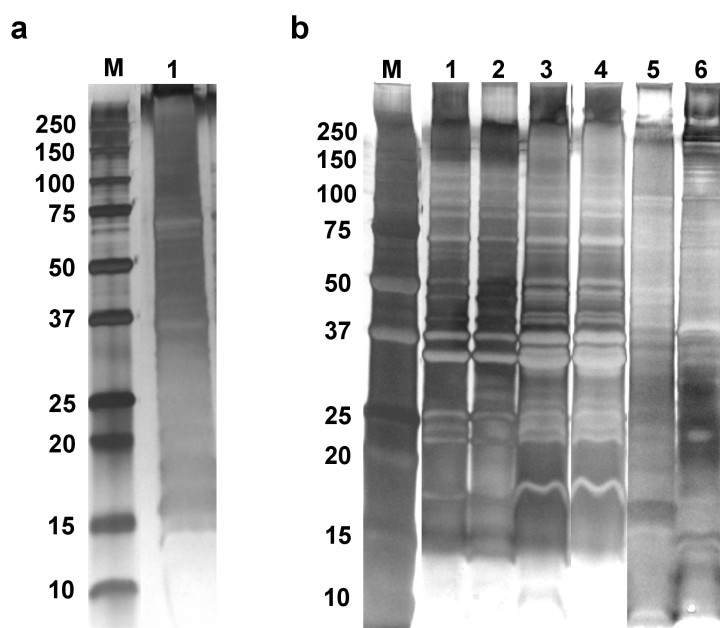
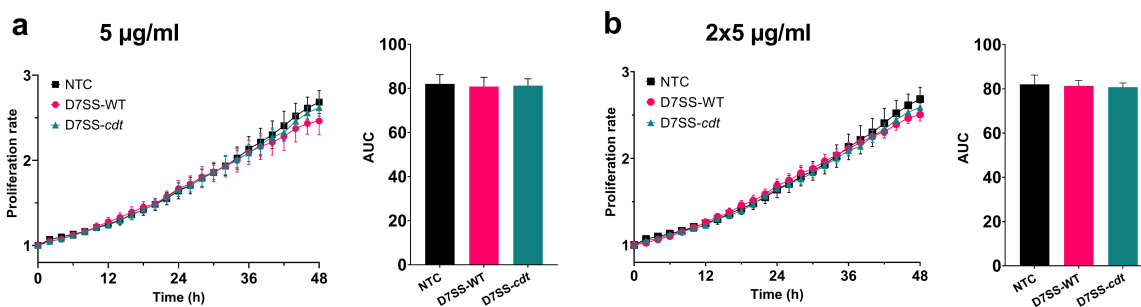
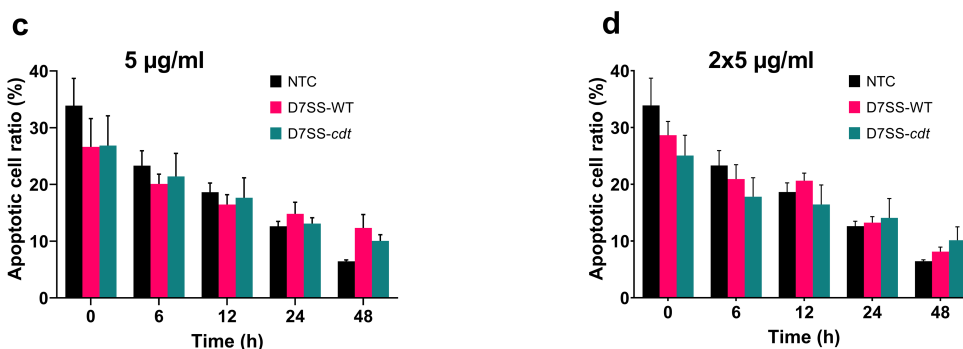


**Fig. S1** SDS-PAGE analysis of EV preparations using silver staining. On the left side are protein sizes (kD) in the pre-stained molecular weight marker (M). **(a)** *P. micra* (1). **(b)** *A. actinomycetemcomitans* D7SS-WT (1). *A. actinomycetemcomitans* D7SS-cdt (2). *A. actinomycetemcomitans* SA3138-WT (3). *A. actinomycetemcomitans* SA3139-LPS-O (4). *P. gingivalis* (5). *F. nucleatum* (6)

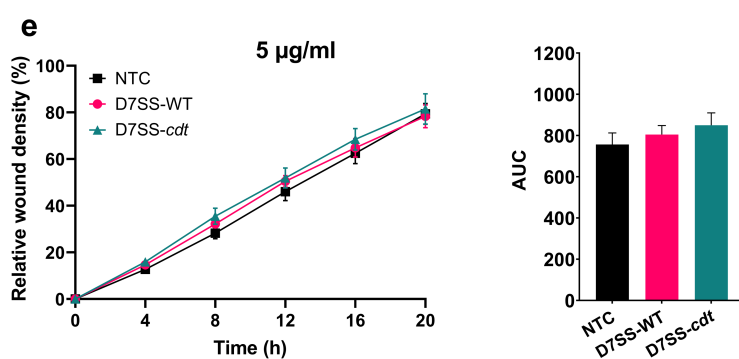
### SCC-24A



### SCC-24A



### SCC-24A



### HSC-3

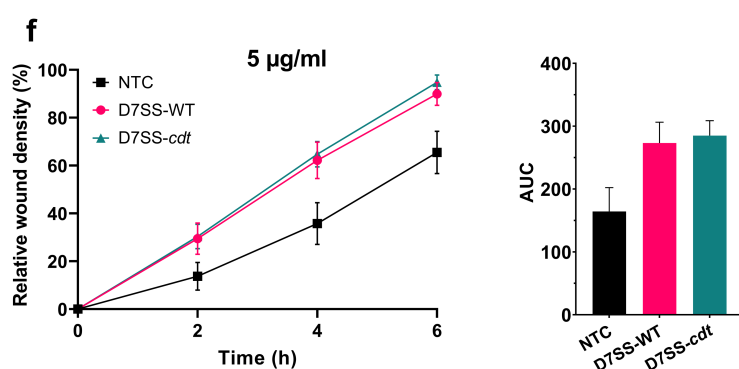
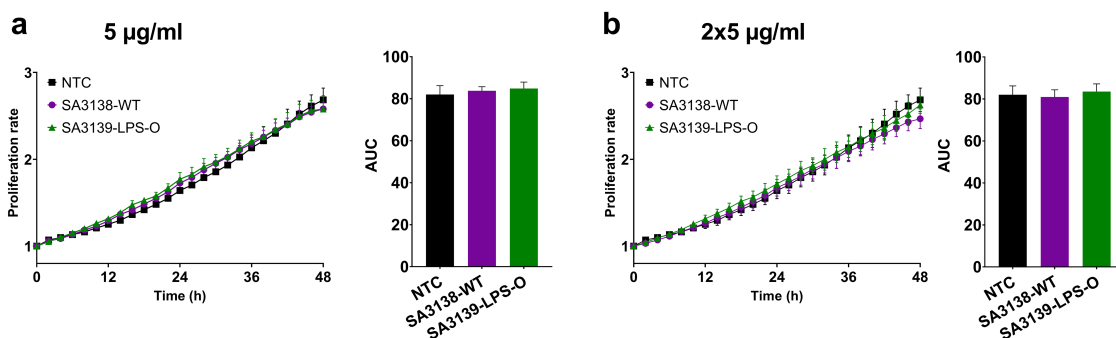


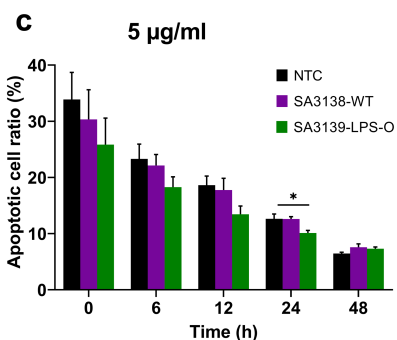
**Fig. S2** Effect of *A. actinomycetemcomitans* D7SS-WT and D7SS-*cdt*-derived EVs on cancer cell proliferation, apoptosis, and migration. **(a-d)** Cell proliferation rates are presented as proliferation rate in relation to time with the corresponding area under the curve (AUC).

Apoptotic cell ratios are shown from representative time points. **(a, b)** EVs (5  $\mu\text{g/ml}$  or  $2 \times 5$   $\mu\text{g/ml}$ ) did not affect the proliferation of SCC-24A cells. **(c, d)** After 48 hours of treatment, EVs might slightly increase the number of apoptotic cells, not statistically significant difference. **(e, f)** Cell migration is presented as the relative wound density over time with the corresponding area under the curve (AUC). **(e)** EVs (5  $\mu\text{g/ml}$ ) did not affect the SCC-24A cell proliferation. **(f)** EVs (5  $\mu\text{g/ml}$ ) might increase the migration of HSC-3 cells but the difference was not statistically significant. Values are shown as mean  $\pm$  SEM. NTC, no treatment control. Experiments were repeated independently three times with triplicates for each condition

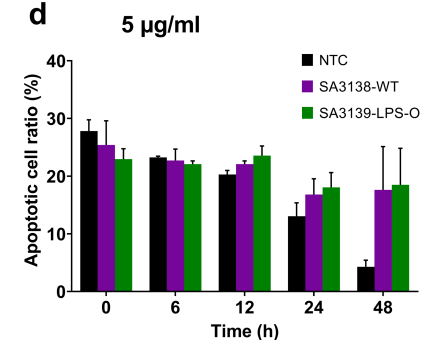
### SCC-24A



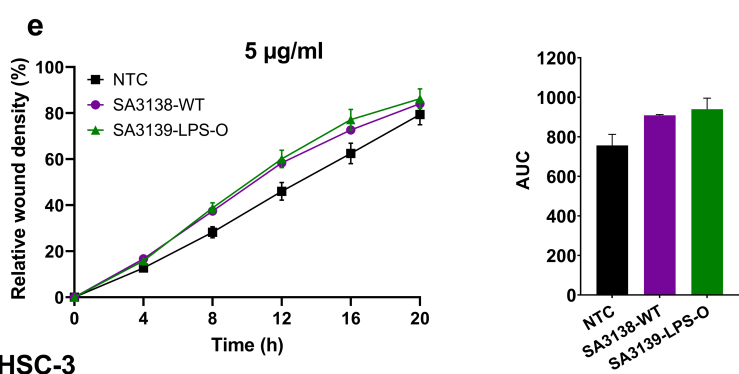
### SCC-24A



### HSC-3



### SCC-24A



### HSC-3

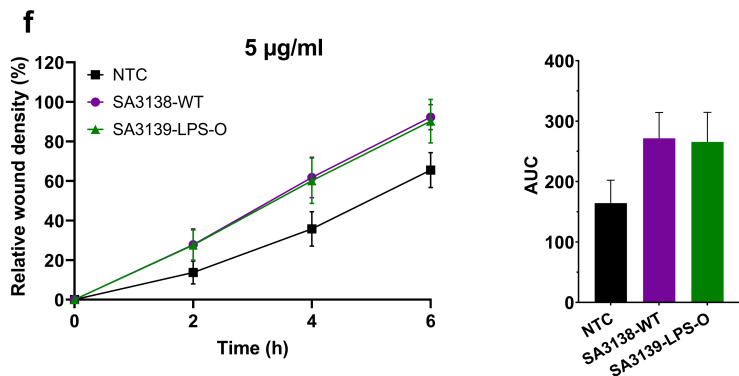


**Fig. S3** Effect of *A. actinomycetemcomitans* SA3138-WT and SA3139-LPS-O-derived EVs on cancer cell proliferation, apoptosis, and migration. **(a-d)** Cell proliferation rates are presented as proliferation rate in relation to time with the corresponding area under the curve (AUC). Apoptotic cell ratios are shown from representative time points. **(a, b)** EVs (5  $\mu\text{g/ml}$  or 2x5

$\mu\text{g/ml}$ ) did not affect the proliferation of SCC-24A cells. **(c)** The number of apoptotic SCC-24A cells was lower at 24 hours following the treatment with SA3139-LPS-O EVs ( $5\mu\text{g/ml}$ ) compared to control cells. **(d)** The metastatic HSC-3 cell apoptosis was increased in cells treated with SA3138 and SA3139-LPS-O EVs ( $5\mu\text{g/ml}$ ) but the difference was not statistically significant. **(e, f)** Cell migration is presented as the relative wound density over time with the corresponding area under the curve (AUC). SCC-24A and HSC-3 cells treated with EVs ( $5\mu\text{g/ml}$ ) derived from SA3138 and SA3139-LPS-O did not show statistically significant increase in cell migration. Values are shown as mean  $\pm$  SEM.  $*P \leq 0.05$ . NTC, no treatment control. Experiments were repeated independently three times with triplicates for each condition.

## SCC-24A

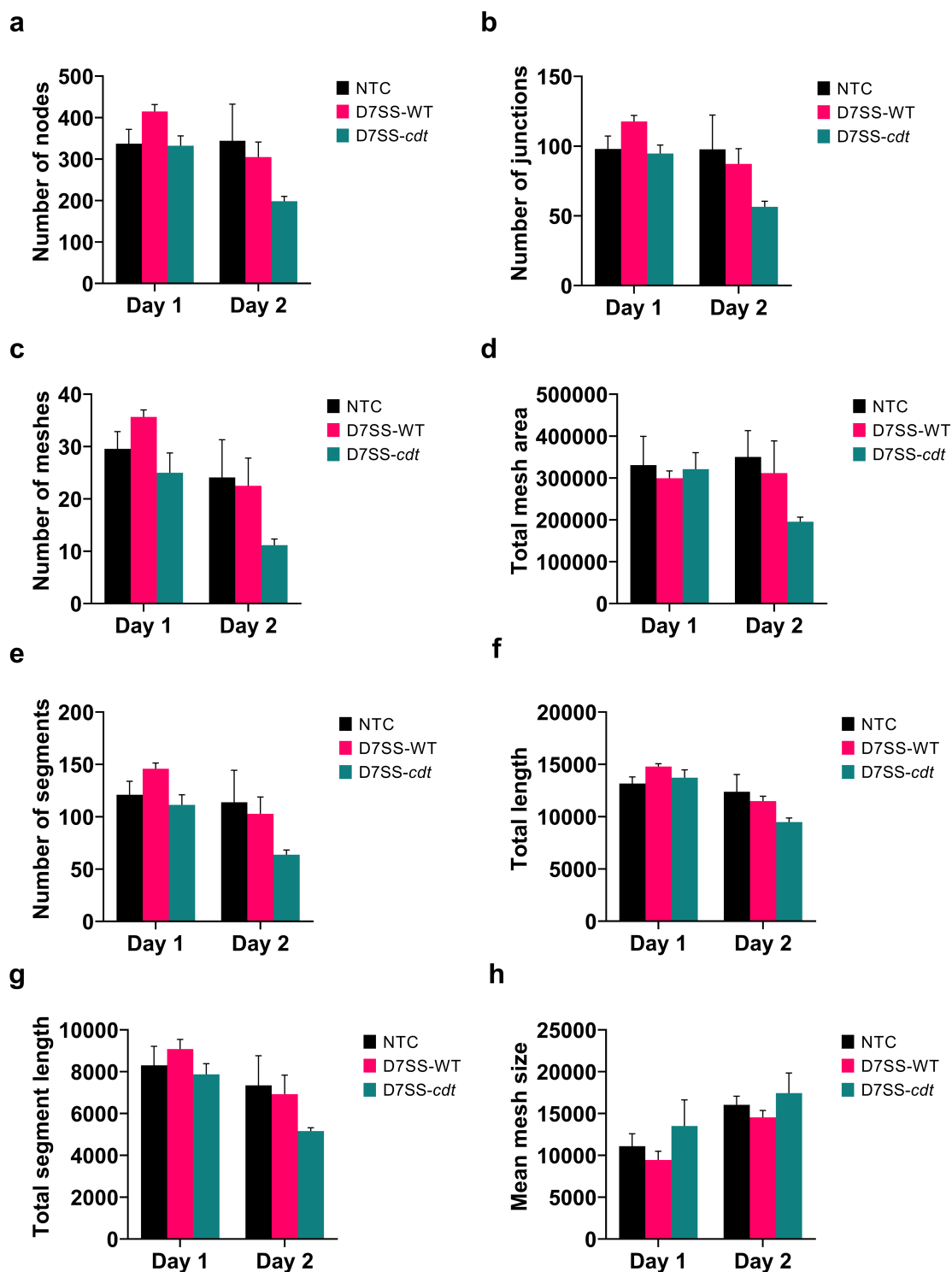


**Fig. S4** Cancer cell-derived tubulogenesis in SCC-24A treated with EVs from *A. actinomycetemcomitans* D7SS-WT and D7SS-cdt. Images were taken on day 1 (8 h) and day 2 (20h). **(a)** Number of nodes. **(b)** Number of junctions. **(c)** Number of meshes. **(d)** Total mesh

area. **(e)** Number of segments. **(f)** Total length. **(g)** Total segment length. **(h)** Mean mesh size.

Values are shown as mean  $\pm$  SEM. NTC, no treatment control. Experiments were repeated independently three times with duplicates for each condition.

## HSC-3

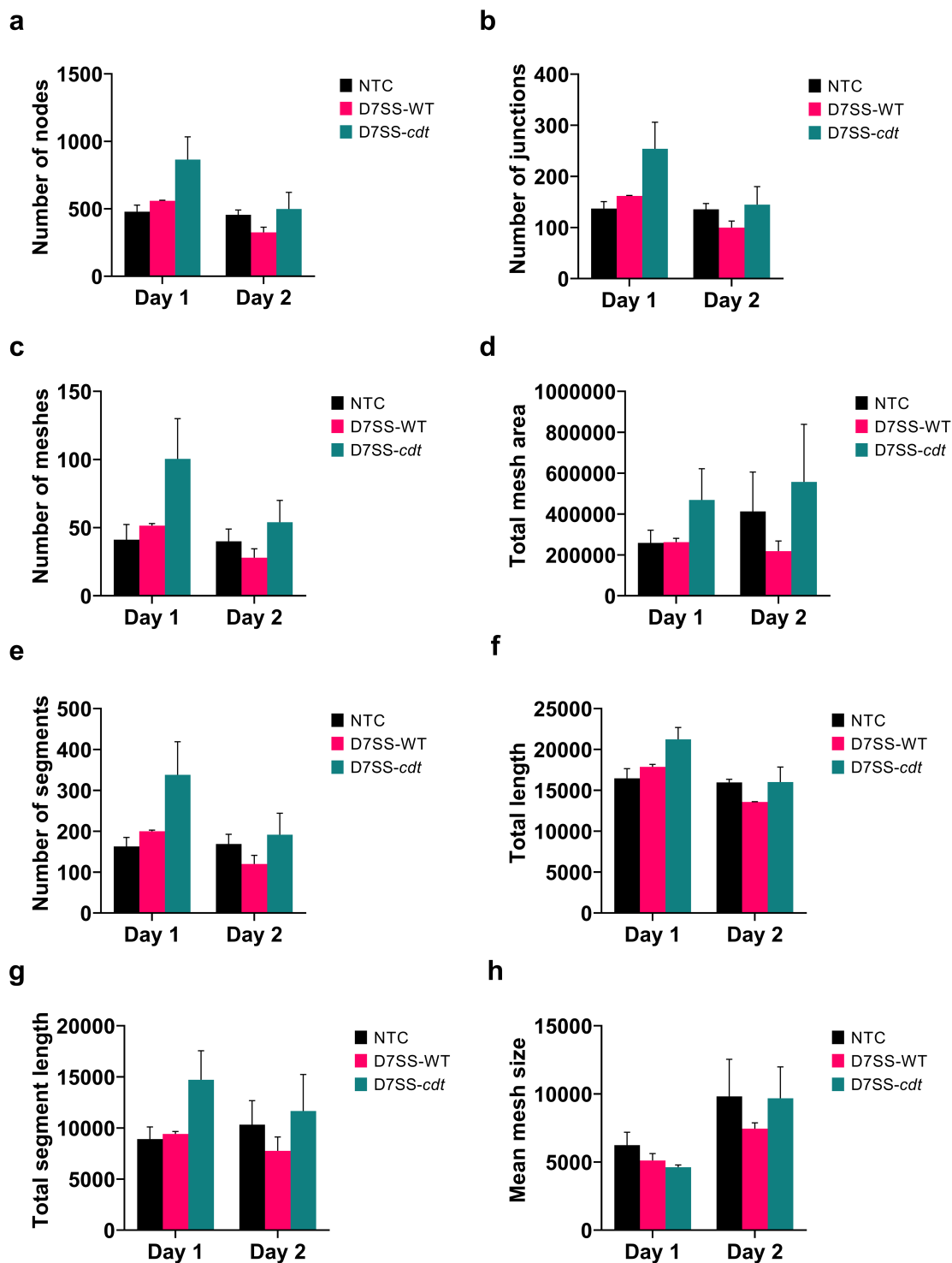


**Fig. S5** Cancer cell-derived tubulogenesis in HSC-3 cells treated with EVs from *A. actinomycetemcomitans* D7SS-WT and D7SS-cdt. Images were taken on day 1 (8 h) and day 2 (20h). **(a)** Number of nodes. **(b)** Number of junctions. **(c)** Number of meshes. **(d)** Total mesh area. **(e)** Number of segments. **(f)** Total length. **(g)** Total segment length. **(h)** Mean mesh size.



Values are shown as mean  $\pm$  SEM. NTC, no treatment control. Experiments were repeated independently three times with duplicates for each condition.

## SCC-24A

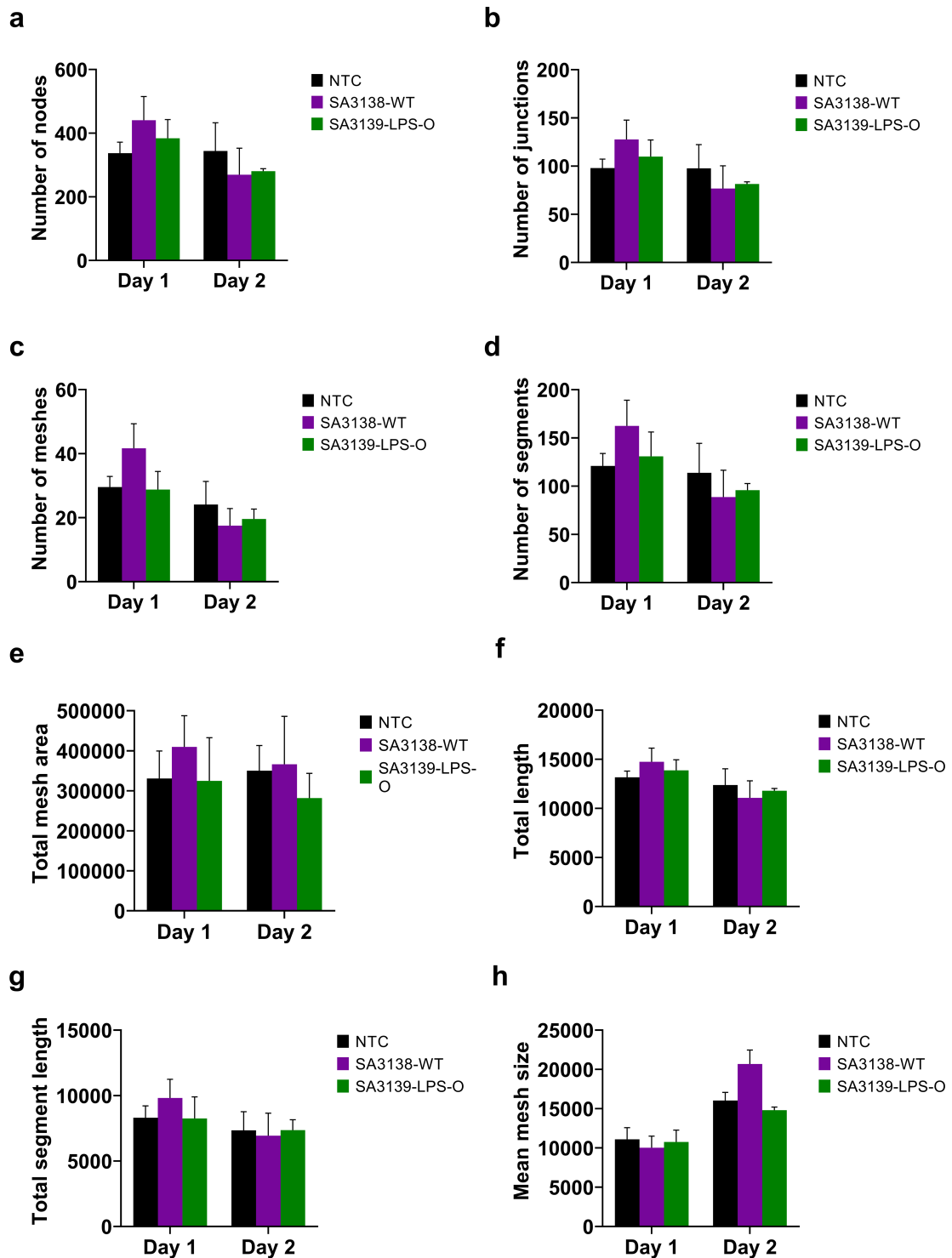


**Fig. S6** Cancer cell-derived tubulogenesis in SCC-24A treated with EVs from *A. actinomycetemcomitans* SA3138-WT and SA3139-LPS-O. Images were taken on day 1 (8 h) and day 2 (20h). **(a)** Number of nodes. **(b)** Number of junctions. **(c)** Number of meshes. **(d)**

Total mesh area. **(e)** Number of segments. **(f)** Total length. **(g)** Total segment length. **(h)** Mean mesh size. Values are shown as mean  $\pm$  SEM. NTC, no treatment control. Experiments were repeated independently three times with duplicates for each condition.

## HSC-3

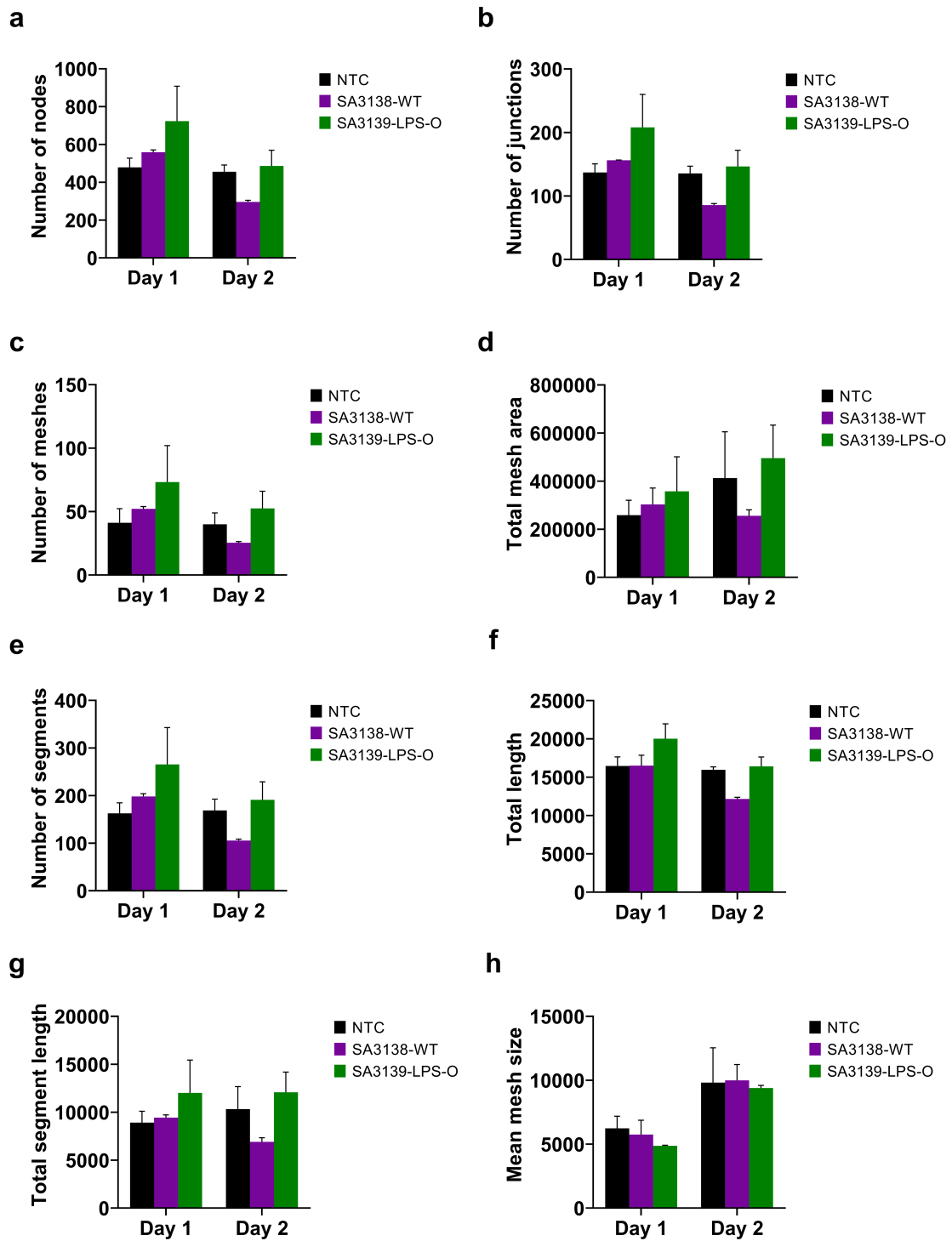
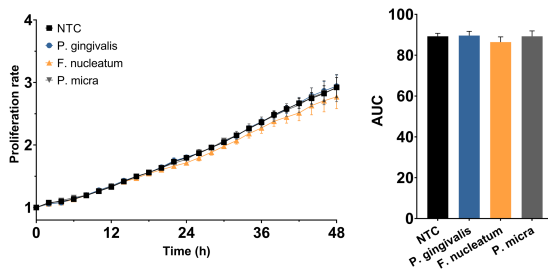


**Fig. S7** Cancer cell-derived tubulogenesis in HSC-3 cells treated with EVs from *A. actinomycetemcomitans* SA3138-WT and SA3139-LPS-O. Images were taken on day 1 (8 h) and day 2 (20h). **(a)** Number of nodes. **(b)** Number of junctions. **(c)** Number of meshes. **(d)** Total mesh area. **(e)** Number of segments. **(f)** Total length. **(g)** Total segment length. **(h)** Mean

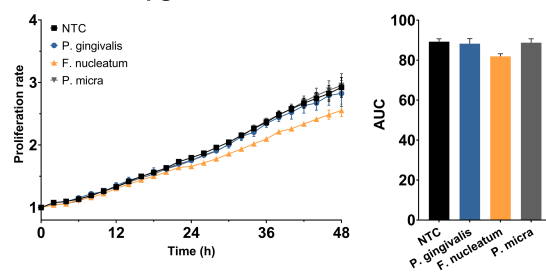
mesh size. Values are shown as mean  $\pm$  SEM. NTC, no treatment control. Experiments were repeated independently three times with duplicates for each condition.

### SCC-24A

**a** 5  $\mu\text{g/ml}$

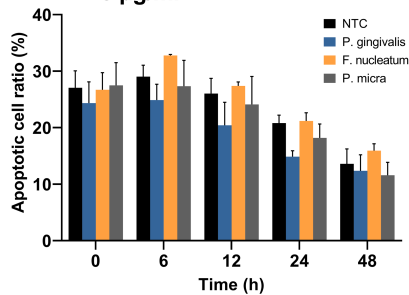


**b** 2x5  $\mu\text{g/ml}$



### SCC-24A

**c** 5  $\mu\text{g/ml}$



### SCC-24A

**d** 5  $\mu\text{g/ml}$

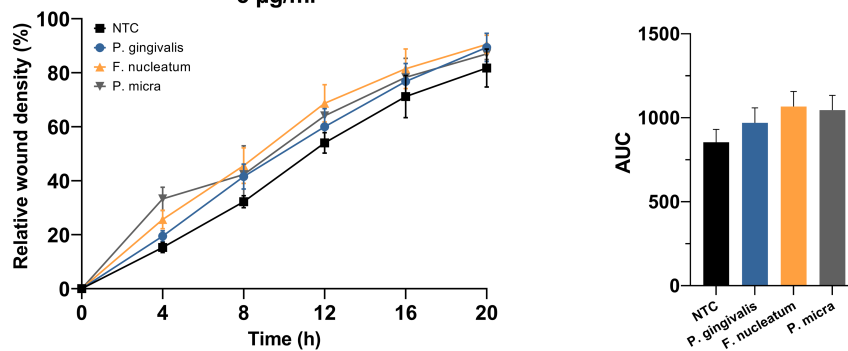


**Fig. S8** Effect of *P. gingivalis*, *F. nucleatum* and *P. micra* -derived EVs on cancer cell proliferation, apoptosis, and migration. **(a-c)** Cell proliferation rates are presented as proliferation rate in relation to time with the corresponding area under the curve (AUC). Apoptotic cell ratios are shown from representative time points. **(a)** EVs (5  $\mu\text{g/ml}$ ) derived from *P. gingivalis*, *F. nucleatum* or *P. micra* did not influence SCC-24A cell proliferation or apoptosis. **(b)** *F. nucleatum* -derived EVs (2x5  $\mu\text{g/ml}$ ) might decrease SCC-24A cell proliferation but the difference was not statistically significant compared to control cells ( $P =$

0.058). **(c)** EVs (5 $\mu$ g/ml) derived from *P. gingivalis*, *F. nucleatum* or *P. micra* did not influence SCC-24A cell apoptosis. **(d)** Cell migration is presented as the relative wound density over time with the corresponding area under the curve (AUC). EVs (5 $\mu$ g/ml) derived from *P. gingivalis*, *F. nucleatum* or *P. micra* did not influence SCC-24A cell migration. Values are shown as mean  $\pm$  SEM. NTC, no treatment control. Experiments were repeated independently three times with triplicates for each condition.